BB-301: a silence and replace AAV-based vector for the treatment of oculopharyngeal muscular dystrophy

Vanessa Strings-Ufombah, Alberto Malerba, Shih-Chu Kao, Sonal Harbaran, Fanny Roth, Ornella Cappellari, Ngoc Lu-Nguyen, Keiko Takahashi, Sophie Mukadam, Georgina Kilfoil, et al.

BB-301: a silence and replace AAV-based vector for the treatment of oculopharyngeal muscular dystrophy

Vanessa Strings-Ufombah,[1,4] Alberto Malerba,[2,4] Shih-Chu Kao,[1] Sonal Harbaran,[1] Fanny Roth,[3] Ornella Cappellari,[2] Ngoc Lu-Nguyen,[2] Keiko Takahashi,[1] Sophie Mukadam,[1] Georgina Kilfoil,[1] Claudia Kloth,[1] Petrus Roelvink,[1] George Dickson,[2,5] Capucine Trollet,[3,5] and David Suhy[1,5]

[1]Benitec Biopharma, Inc., Hayward, CA 94545, USA; [2]Department of Biological Sciences, School of Life Sciences and the Environment, Royal Holloway University of London, Egham, Surrey TW20 0EX, UK; [3]Sorbonne Université, INSERM, Association Institut de Myologie, Centre de Recherche en Myologie, 75013 Paris, France

Oculopharyngeal muscular dystrophy (OPMD) is a rare autosomal dominant disease that results from an alanine expansion in the N-terminal domain of Poly-A Binding Protein Nuclear-1 (PABPN1). We have recently demonstrated that a two-vector gene therapy strategy significantly ameliorated the pathology in a mouse model of OPMD. This approach entailed intramuscular injection of two recombinant adeno-associated viruses (AAVs), one expressing three short hairpin RNAs (shRNAs) to silence both mutant and wild-type PABPN1 and one expressing a codon-optimized version of PABPN1 that is insensitive to RNA interference. Here we report the continued development of this therapeutic strategy by delivering "silence and replace" sequences in a single AAV vector named BB-301. This construct is composed of a modified AAV serotype 9 (AAV9) capsid that expresses a unique single bifunctional construct under the control of the muscle-specific Spc5-12 promoter for the co-expression of both the codon-optimized PABPN1 protein and two small inhibitory RNAs (siRNAs) against PABPN1 modeled into microRNA (miRNA) backbones. A single intramuscular injection of BB-301 results in robust inhibition of mutant PABPN1 and concomitant replacement of the codon-optimized PABPN1 protein. The treatment restores muscle strength and muscle weight to wild-type levels as well as improving other physiological hallmarks of the disease in a mouse model of OPMD.

INTRODUCTION

Oculopharyngeal muscular dystrophy (OPMD) is a rare, autosomal-dominant, slow-progressing neuromuscular disorder that first manifests in midlife, advances with age, and is characterized by progressive ptosis, swallowing difficulties, and proximal limb weakness. OPMD affects the function of all muscle groups. Among these are dysphagia-related complications that are caused by weakness in the tongue and pharynx muscles and most often require severe intervention.[1,2] OPMD is characterized by complications such as choking, regurgitation, aspiration pneumonia, poor nutrition, and social withdrawal, which often result in severely impaired quality of life.[3]

OPMD is caused by a polyalanine expansion mutation in the gene encoding polyadenylate RNA binding protein nuclear 1 (PABPN1),[4] a ubiquitously expressed protein that functions as a regulator of mRNA stability.[5] The N terminus of the wild-type PABPN1 protein typically contains a tract of 10 alanine residues. The mutant PABPN1 gene has a repeat GCG expansion mutation that results in a PABPN1 protein with a N-terminal polyalanine tract of up to 18 contiguous alanine residues,[4,6] which is prone to form aggregates called intranuclear inclusions (INIs) in muscle cells.[7,8] The role of these aggregates, as is the case in many neurodegenerative diseases, is still controversial, but recent studies have suggested that INIs that also sequester wild-type PABPN1 could contribute to the loss-of-function phenotype associated with OPMD.[5,9–11]

We have previously demonstrated the efficacy of a two-vector adeno-associated virus (AAV)-based gene therapy strategy to correct mutant phenotypes in the A17 mouse, the most common murine model of OPMD.[12] This model is generated in the Friend leukemia virus B (FvB) background by overexpressing a bovine expanded (17 alanine residues) copy of PABPN1 and displays many of the overt clinical signs observed in human OPMD patients including the presence of INIs, fibrosis in affected muscles, and loss of muscle strength.[3,13,14] In our previous study, the two recombinant AAV vectors were comprised of (1) a recombinant AAV serotype 8 (AAV8) producing small inhibitory RNA (siRNAs) to silence endogenous (mutant and wild-type) PABPN1 and (2) an AAV9 vector expressing a codon-optimized version of wild-type PABPN1 (coPABPN1) that takes advantage of amino acid codon degeneracy to produce the wild-type PABPN1 protein from a mRNA that is not targeted by the anti-PABPN1 siRNAs. Although single
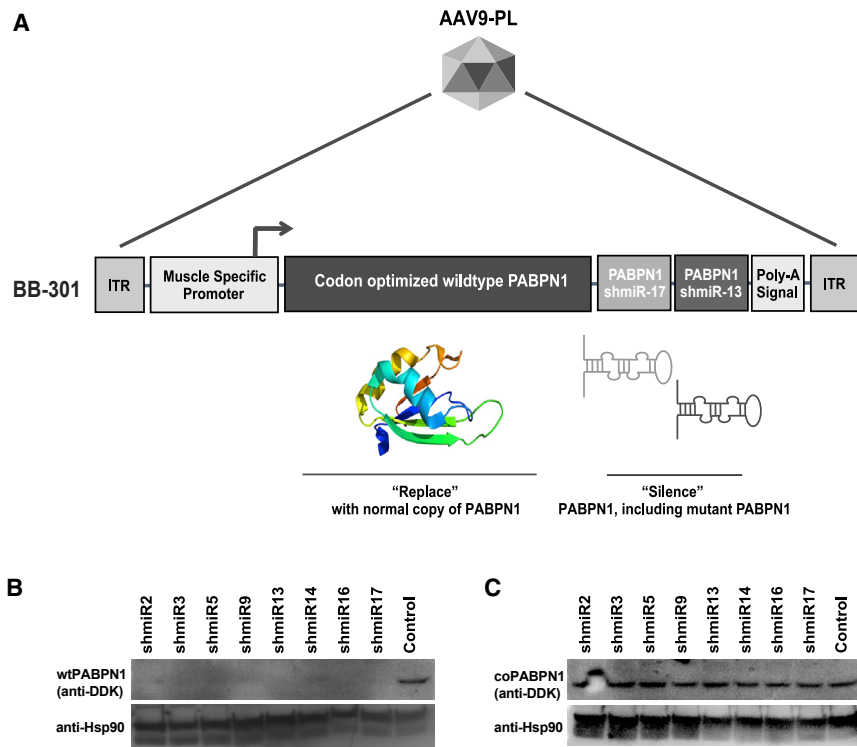
A

Figure 1. BB-301 delivers two shmiRs and expresses human codon-optimized PABPN1 resistant to degradation by shmiRs

(A) Muscle-specific promoter Spc5-12 drives the expression of codon-optimized wild-type PABPN1 and shmiR17 and shmiR13, which target both mutant and wild-type PABPN1 with high efficiency. The shmiRs are followed by a terminator sequence and a polyA tailing sequence. The shmiRs are unable to target the codon-optimized PABPN1. (B) The efficacy of each shmiR was assessed by western blot analysis against PABPN1. Cells were co-transfected with each shmiR and a plasmid expressing wild-type PABPN1 linked to FLAG-tag (ddk). As a negative control, an unrelated plasmid, pSilencer, was transfected. All shmiRs tested were able to reduce PABPN1 expression. (C) The ability of the shmiRs to reduce codon-optimized PABPN1 protein expression was also evaluated. Cells were co-transfected with each shmiR and a plasmid expressing codon-optimized PABPN1 (coPABPN1) linked to FLAG-tag (ddk). All shmiRs were unable to affect coPABPN1 levels. The unrelated protein (Hsp90) expression level was not affected by any of the shmiRs.

administration of either of the two vectors resulted in a partial improvement of the mutant phenotypes, only when both vectors were administered simultaneously did improvement result in restoration of muscle strength to wild-type levels. A two-vector approach for human therapeutic applications is undesirable, as it would require two independent manufacturing processes, which can significantly increase costs, technical risk, and potential regulatory challenges.

Here, we describe the development of BB-301, which combines the essential elements of the two vectors into a single "silence and replace" recombinant AAV vector. In this construct the Spc5-12 muscle-specific promoter drives the expression of a unique bifunctional RNA that co-expresses the codon-optimized coPABPN1 sequence as well as the siRNAs suppressing endogenous mutant and wild-type PABPN1. A dose escalation study in the A17 mouse model was performed over 14 weeks to evaluate the activity of BB-301 as single doses administered at 4×10^8 to 7.5×10^{11} vector genomes (vg)/muscle. Mid-range doses of BB-301 resulted in 75% inhibition of mutant PABPN1 and 26% restoration of wild-type PABPN1 activity leading to full restoration of muscle strength and muscle weight as well as clearance of INIs and a reduction of fibrosis. In a follow-on 20-week time course experiment, we demonstrate that a suboptimal dose of BB-301 that achieves partial resolution at week 14 can still achieve significant benefit, albeit at a slower rate than higher doses, as evidenced by full restoration of muscle strength, weight, and the

aggregate formation associated with disease pathology in the A17 model.

RESULTS

Generation and design of the BB-301 vector

Our previous studies demonstrated the efficacy of a two-vector AAV-based gene therapy strategy to correct mutant phenotypes in the A17 mouse.[12] However, using two independent AAV vectors is not ideal from a regulatory and manufacturing standpoint for a clinical-stage therapy. Therefore, we generated BB-301, a recombinant AAV vector that includes both the "silence" and "replace" functions of our previously described two-vector system in a single construct. The vector has the synthetic muscle-specific Spc5-12 promoter[15,16] that drives the expression of a bifunctional mRNA transcript encoding the human codon-optimized PABPN1 as well as siRNA sequences targeting both the endogenous and mutant PABPN1 (Figure 1A) followed by the transcriptional terminator and a polyA tailing sequence derived from the bovine growth hormone gene. The expressed bifunctional mRNA serves as a substrate for ribonuclease III enzymes that recognize the presence of the anti-PABPN1 siRNAs embedded in microRNA (miRNA) backbones (shmiRs) in the 3′ end of the transcript, excising them to convert the moieties into functional siRNAs. The siRNA sequences ultimately produced from BB-301 were designed to target conserved regions across murine, human, and bovine sequences. The remaining mRNA transcript is translated to produce the codon-optimized PABPN1 protein, which has the same amino

acid sequence as the endogenous wtPABPN1 protein albeit encoded by a different nucleic acid sequence (sequence listed in Table S1).

BB-301 contains AAV2-derived inverted terminal repeat (ITR) sequences for gene replication and uses a modified version of the AAV9 capsid for delivery, termed AAV9 phospholipase (AAV9PL). We have observed that the baculovirus insect cell system was able to produce unmodified AAV9 vector with very high yield. However, the infectivity of these AAV9 vectors was substantially lower than those generated by the mammalian 293 cell system. Based on literature review and analysis of amino acid sequence, we hypothesized that this was likely due to a malfunction of the phospholipase activity that enables the AAV to escape from endosomes inside the cell.[17,18] Interestingly, the serotype AAV2 produces functional progeny in both mammalian and insect cell cultures.[18] The AAV2 phospholipase sequence differs in 5 amino acids from the AAV9 phospholipase sequence. Therefore, we introduced these 5 amino acid substitutions at specific sites within the AAV9 phospholipase domain in the VP1 capsid protein that changed the sequence into the AAV2 phospholipase sequence and thus restored the phospholipase activity in the AAV9 capsid. We have found that in the baculovirus insect cell manufacturing system such restoration of the phospholipase domain is essential for the production of highly infective and functional AAV9 vectors.

Previously, we have demonstrated that perfect stem loop structures produce a large heterogeneity of mature siRNA sequences due to inefficient loop processing by ribonuclease III-like enzymes.[19] Thus, instead of expressing shRNA with perfect complementary base pairing in the stem structure, BB-301 was configured to produce hybrid molecules that we term shmiRs. By embedding the two siRNA sequences into endogenous miRNA backbones, the transcripts are processed like endogenous miRNA, which generally results in the production of 1 or 2 predominant mature siRNA species. This will likely reduce off-target effects and produce a more consistent pool of siRNAs for the intended therapeutic benefit.[20]

Next-generation sequencing (NGS) was performed to demonstrate that the processing of each of the two shmiRs produced by BB-301 generates either one or two predominant siRNA products (Figure S1A). Furthermore, each of the resulting products from processing of the shmiRs had high levels of inhibitory activity when tested as mature siRNA in a tissue culture model (Figure S1B). Within the context of the expressed siRNA sequences (listed in Table S2), inhibitory activity was determined independently by co-transfecting HEK293 cells with an anti-PABPN1 shmiR expression construct as well as a PABPN1 expression construct (wtPABPN1) in which the 3X-FLAG-tag fusion sequence is expressed at the C terminus of the wild-type protein. Seventy-two hours post-transfection, PABPN1 protein expression levels were determined by western blot analysis. All tested shmiRs provided substantial PABPN1 inhibition, whereas an unrelated protein (HSP90) was not changed by shmiR expression (Figure 1B). A similar experiment was performed to demonstrate that the shmiRs do not inhibit expression of the codon-optimized PABPN1 (coPABPN1). HEK293 cells were co-transfected with individual shmiR expression constructs and a plasmid expressing co-PABPN1 that contained a 3X-FLAG-tag epitope. As predicted, the shmiRs do not recognize the coPABPN1 sequence (Figure 1C).

In addition, all of the shmiRs were tested for their hyperfunctionality to inhibit PABPN1 expression in a luciferase reporter assay. A serial dilution of shmiR constructs was co-transfected with a luciferase reporter that contains PABPN1 coding sequence fused to a luciferase reporter gene into HEK293 cells. As shown in Figure S2A, all of the shmiRs were able to inhibit expression of the fused PABPN1-luciferase transcripts >85% at low concentrations (100 ng, equivalent of 0.05 pmol). shmiR3, shmiR13, and shmiR14 showed greater hyperfunctional activities than the other shmiRs, with 30% inhibition remaining at 0.02 ng (equivalent of 0.01 fmol) concentration.

Upon BLAST search of individual shmiR target sequences against human genomic and transcript databases, shmiR3, shmiR14, shmiR13, and shmiR17 had the fewest potential off-targets and were chosen for further testing. The final four shmiRs were tested in various combinations to select for the most efficient PABPN1 knockdown. Mouse C2C12 cells were electroporated with different combinations of shmiRs. Inhibition of endogenous PABPN1 expression was examined by quantitative reverse-transcriptase PCR (qRT-PCR) analysis. The combination of shmiR13 and shmiR17 showed the most inhibition of PABPN1 and high activity at the lowest picomolar concentrations compared with the other combinations of shmiRs, leading to the decision of using the combination of shmiR13 and shmiR17 in the BB-301 construct (Figure S2B). These data demonstrate that BB-301 efficiently downregulates endogenous PABPN1 in an *in vitro* system, while simultaneously expressing a human codon-optimized version of PABPN1 resistant to the degradation by the concomitantly expressed shmiR sequences.

BB-301 expression profile and efficacy in restoring muscle strength and INI clearance in muscles of A17 mouse model

To assess the ability of the BB-301 vector to restore phenotypic parameters associated with OPMD, a dose escalation study was performed in A17 mice. BB-301 was injected into the *tibialis anterior* (TA) muscles of 10- to 12-week-old A17 mice at six different doses ranging from 4×10^8 to 7.5×10^{11} vg/muscle. Saline-treated TA muscles of age-matched A17 mice or FvB parental-strain animals served as negative controls. At 14 weeks post-BB-301 administration, mice were anesthetized and contractile properties of TA muscles were analyzed by *in situ* muscle electrophysiology.[21]

The impact of BB-301 on the restoration of muscle strength in the TA muscle was assessed by muscle contractility measurements in response to a series of induced impulses that ranged from 10 to 180 Hz. Dependent on whether a single or multiple time points were analyzed, either 2-way ANOVA or mixed-effects analysis (Figure 5), to account for repeated measures, was applied. At the 150 Hz frequency, the maximal contractility force in A17 mice was reduced by 35% compared with their wild-type FvB counterparts (800 mN versus 1,150 mN, respectively, $p < 0.001$) (Figure 2A). The doses ranging from 4×10^8 vg/muscle to
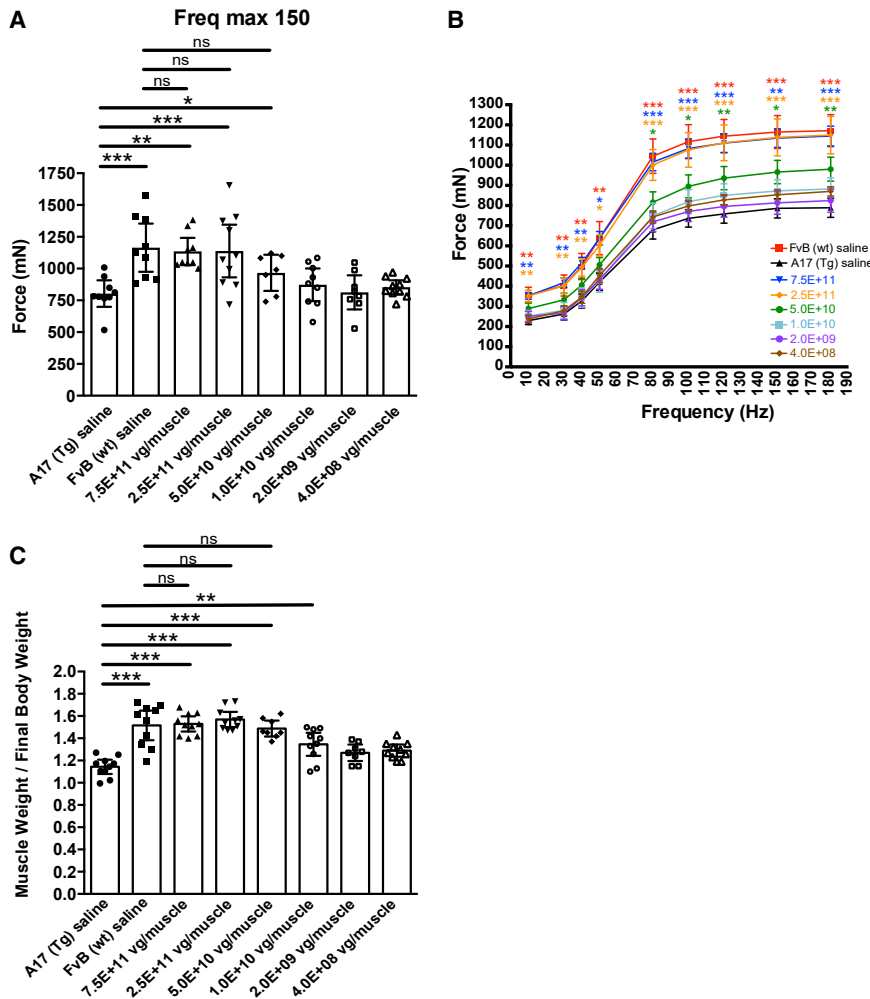
A

Freq max 150

B

C

Figure 2. Increase in muscle strength correlates with increase in muscle weight after dose-dependent administration of BB-301 in A17 mice

(A) Maximal force generated by TA muscles of BB-301-treated mice was measured by *in situ* muscle physiology: the three highest doses significantly increased the maximal force generated by TA muscles as measured at 150 Hz. (B) Maximal force generated by TA muscles of BB-301-treated mice in response to a set of different stimulations (10–180 Hz) at 14 weeks was measured by *in situ* muscle physiology. The three highest doses significantly increased the maximal force generated by TA muscles. The color of the asterisks refers to the comparison of the BB-301-treated versus A17-saline injected muscles. (C) Fourteen weeks after AAV administration, an apparent dose-dependent increase in muscle weight was observed for BB-301-treated compared with saline-treated TA muscles of A17 mice. Data are presented as mean ± 95% confidence interval. Sample size ranged from 7 to 10 TA muscles per dosing group as indicated by the dot plot. Two-way ANOVA analysis with Tukey multiple comparison test was used for data analysis. *$p < 0.05$, **$p < 0.01$, ***$p < 0.001$; ns, not significant.

per cell. Dose-dependent production of both anti-PABPN1 siRNA13 and siRNA17 was verified in TA muscles (Figure 3A). Animals treated with the lowest dose of 4×10^8 vg/muscle showed no detectable production of siRNA above the background of the assay. At higher doses, siRNA was measurable in increasing quantities, with 2.4×10^6 copies of siRNA13 and 1.7×10^6 copies of siRNA17 per input of 50 ng of RNA. qRT-PCR analysis was used to verify corresponding knockdown of PABPN1 mRNA levels. This analysis detected both endogenous wild-type PABPN1 transcript and the mutant PABPN1 transcript but does not recognize or amplify sequences corresponding to the transduced codon-optimized PABPN1 mRNA species. Low levels of PABPN1 mRNA inhibition (∼14%) were observed in muscles dosed with 2×10^9 vg/muscle, corresponding to ∼2,500 copies of each siRNA per 50 ng of input RNA (Figure 3B). Moderate doses of 1×10^{10} and 5×10^{10} vg/muscle resulted in inhibition of ∼31%, while higher doses resulted in >75% inhibition of PABPN1. Likewise, qRT-PCR analyses using primers designed to selectively amplify codon-optimized PABPN1 sequences were performed (Figure 3C). These additional qRT-PCR analyses demonstrated that BB-301-treated muscles expressed codon-optimized PABPN1 at levels ranging from 1% to 63% of normal levels when tested at 14 weeks post-transduction. Collectively, the analyses in Figure 3 confirm that BB-301 can produce siRNAs that have the capability to knock down endogenous PABPN1 wild-type and mutant transcripts in the A17 mouse model while simultaneously expressing a codon-optimized version of PABPN1.

1×10^{10} vg/muscle showed only minor improvement in maximal force at 14 weeks post-dosing. The 5×10^{10} vg/muscle dose showed significant improvement ($p < 0.05$) resulting in ∼50% restoration in maximal force. The top two doses, 2.5×10^{11} vg/muscle and 7.5×10^{11} vg/muscle, led to a complete restoration in maximal force ($p < 0.001$) (Figure 2B).

After the strength analysis *in situ*, the TA muscles were collected for additional evaluation including muscle weight, histology, and molecular analyses. Regarding muscle weight, TA muscles from A17 mice weigh ∼25% less than the same muscles in FvB wild-type mice ($p < 0.001$) The increase in maximal force for the three highest dose-treated muscles correlated well with an increase in muscle mass and muscle mass normalized to wild-type levels ($p < 0.01$ for 5×10^{10} vg/muscle and $p < 0.001$ for 2.5×10^{11} and 7.5×10^{11} vg/muscle) (Figure 2C).

To verify siRNA production, RNA isolated from TA muscles was evaluated by qRT-PCR analysis using methodologies that have the capability to quantitatively detect RNA templates within 100 copies
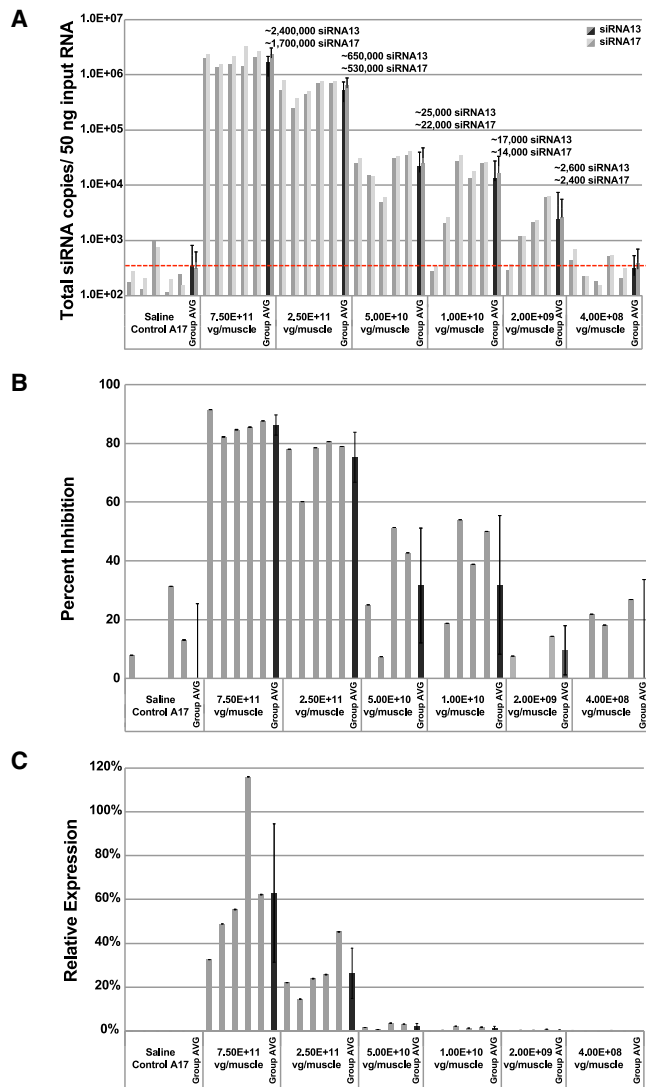
Figure 3. Dose-dependent administration of BB-301 in A17 mice correlates with siRNA expression, endogenous PABPN1 inhibition, and coPABPN1 expression

A17 animals were injected intramuscularly with BB-301. Fourteen weeks post-administration, treated muscles were collected and processed to analyze siRNA copy number, coPABPN1 expression, and inhibition of endogenous PABPN1 via qRT-PCR. (A) Total siRNA copies detected in treated muscles. Individual animals are shown in gray and light gray; group averages from each cohort are shown in black and dark gray. The dotted red line indicates the lower limit of quantitation (LLOQ) of the qRT-PCR assay for siRNA copy detection. (B) PABPN1 inhibition. Individual animals are shown in dark gray; group averages from each cohort are shown in black. (C) Relative expression of coPABPN1. Individual animals are shown in gray; group averages from each cohort are shown in black. Data are presented as mean ± standard deviation (SD).

BB-301 treatment restores normal physiology in A17 muscles

The effects of BB-301 treatment of muscles were assessed by the examination of histological abnormalities associated with the A17 mice. INIs are known to be present within the animals at the time

of dosing with BB-301. After BB-301 treatment, there was a dose-dependent reduction of INIs, with the lowest dose of 4×10^8 vg/muscle providing no or minimal effect on INI formation in muscle cells while highest doses substantially cleared and resolved the aggregates to 2%–5% of initially present INI (p < 0.001) (Figures 4A and 4B).

The impact of the dose response on PABPN1 inhibition and codon-optimized PABPN1 expression is summarized in Table 1. These data suggest that modest restoration of strength (at the 5×10^{10} vg/muscle dose) occurs at 31% PABPN1 inhibition when coupled with co-PABPN1 mRNA expression at 2% of normal levels. The next highest dose of 2.5×10^{11} vg/muscle resulted in complete maximal force restoration despite modest levels of inhibition (75%) and codon-optimized mRNA expression (26%). Cumulatively, these data suggest that a partial knockdown and replacement may be sufficient to significantly reduce the percentage of nuclei with INI and improve disease phenotype by increasing muscle weight and function, suggesting benefit over a broad range of doses.

Suboptimal dosing of BB-301 in A17 mice can achieve a significant impact at a longer time point

To determine whether a longer duration of treatment with BB-301 would improve its efficacy, a suboptimal dose of 1×10^{10} vg/muscle was administered into each TA and muscles were assessed post-dosing at either week 14 or week 20. A significant reduction in the number of INIs was observed at both time points, suggesting that 14 weeks is sufficient to achieve the highest degree of INI clearance and that INI clearance precedes improvements in muscle function (Figures 5A and 5B). Measurement of muscle strength at 14 and 20 weeks showed that increasing the duration of muscle exposure to BB-301 resulted in improved muscle strength, with maximal force generated after 20 weeks higher than at 14 weeks (Figure 5C). Similarly, these data correlated with both the increase in muscle weight (Figure 5D) and muscle cross-sectional area (Figure 5E) that were significantly higher than in saline-treated A17 muscles only 20 weeks after injection. These data suggest that even suboptimal doses of BB-301 may provide full functional improvement if given a longer duration of time to demonstrate improvement, suggesting that the reversal of the diseased phenotypes can be both dose and time dependent.

DISCUSSION

There is currently no efficacious treatment available for patients affected by OPMD. We recently demonstrated that a gene therapy approach using two distinct AAV vectors is an effective treatment for OPMD in the A17 mouse model. Here we show that BB-301, a single "silence and replace" gene therapy agent, has promising potential as a treatment for patients with OPMD. Targeted, viral-based gene therapies have gained momentum for their potential to correct genetic diseases. The field has evolved to include viral vectors with payloads that extend beyond simple protein replacement. In particular, there are likely a wide variety of genetic disorders, such as other trinucleotide expansion diseases, in which one must first knock out or inhibit the autosomal dominant gain-of-function activity. Viral vectors, and especially AAV-derived vectors, have limited packaging capacity, which makes
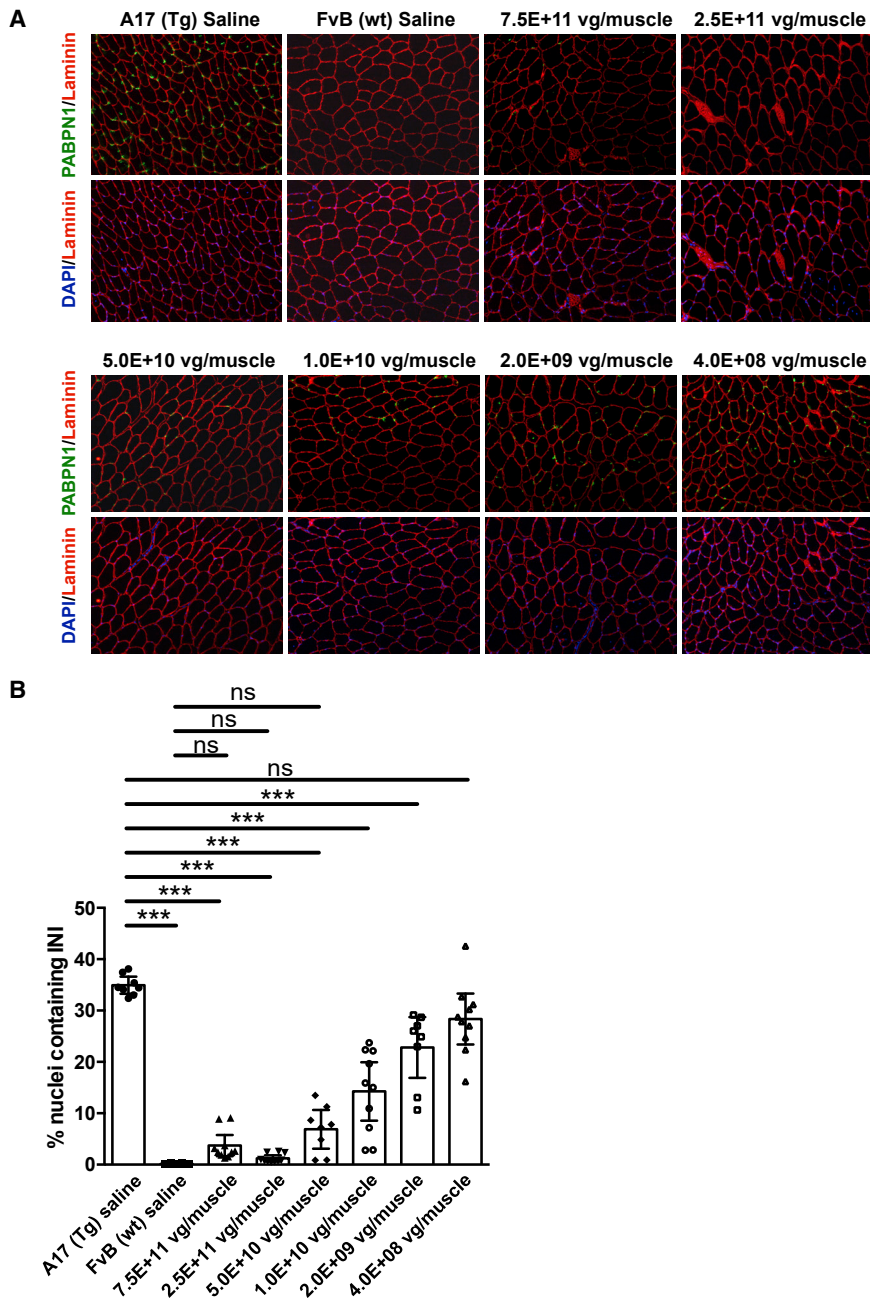
Figure 4. BB-301 administration reduces INI in TA muscles of A17 mice

(A) Detection of PABPN1 (green) and laminin (red) by immunofluorescence in sections of BB-301-treated muscles from the A17 mouse and in saline-injected muscles. An untreated negative control FvB is included for comparison. Sections were pre-treated with 1 M KCl to remove all soluble aggregates from the tissue. (B) Quantification of percentage of nuclei containing INIs in muscle sections indicates that treatment with higher doses of BB-301 efficiently reduces INIs by ~70% compared with saline-injected A17 mice. Injection of lower doses also significantly reduces the INI levels but is somewhat less effective. Only the lowest dose (4×10^8 vg/TA muscle) did not significantly decrease INI content. Data are presented as mean ± 95% confidence interval. Sample size ranged from 8 to 10 TA muscles per dosing group as indicated by the dot plot. Two-way ANOVA analysis with Tukey multiple comparison test was used for data analysis. At doses up to 1×10^{10} vg/muscle, $p < 0.0001$; at the dose of 2×10^9 vg/muscle, $p = 0.0004$; and at the dose of 4×10^8 vg/muscle, $p = 0.1438$. ***$p < 0.001$; ns, not significant.

each species. Therefore, there is plenty of packaging capacity remaining within the same recombinant vector to allow for expression of small to medium size proteins. By positioning the shmiRs in the 3' end of the transcript, these inhibitory sequences can be excised from the nascent transcript while leaving the 5' capped end intact to be fed into the host cell translational machinery. Codon optimization of the gene encoding the replacement protein ensures that there is no change in amino acid composition. Concurrently, changing the nucleotide targeted sequences in the codon-optimized gene ensures that the shmiR sequences do not prevent the remainder of the transcript from producing PABPN1. A similar approach has been employed for the treatment of alpha-1 antitrypsin deficiency[22,23] and for a rhodopsin gene therapy to treat retinitis pigmentosa.[24]

The use of siRNA/miRNA hybrids, termed shmiRs, results in enhanced safety and specificity. We have previously demonstrated that "perfect" complementary hairpins get processed by cellular RNase III-like enzymes at many different positions. In addition, there can be variability in the 5' end or 3' end of the shRNA as a result of differential transcriptional initiation or transcriptional termination, respectively. NGS analyses revealed that a single "perfect" shRNA can be differentially processed and results in dozens of mature siRNA species, which may produce off-target effects or result in a heterogeneous pool, with each siRNA species having differential inhibitory activity.[19] The miRNA backbone

it difficult to envision how multiple therapeutic modalities can be delivered to target tissues or organs with fewer than two, or more, viral vectors that must then be simultaneously administered.

With BB-301, a "silence and replace" vector, we achieve a therapeutic effect by combining silencing siRNA sequences (in miRNA backbones) that target wild-type and mutant messengers of an aberrant gene with replacement gene sequences for a codon-optimized version of endogenous protein. The sequences that encode the shmiRs are ~115 bases for

Table 1. Dose-dependent effect of BB-301 on PABPN1 inhibition and codon-optimized PABPN1 expression (mean ± SD)

BB-301 dose (vg)	"Silence" inhibition PABPN1 (%)	"Replace" coPABPN1 expression (%)
7.50E+11	86.3 ± 3.5	63.0 ± 31.6
2.50E+11	75.2 ± 8.5	26.2 ± 11.4
5.00E+10	31.6 ± 19.5	2.2 ± 1.3
1.00E+10	31.8 ± 23.6	1.1 ± 0.9
2.00E+09	9.6 ± 8.4	0.3 ± 0.3
4.00E+08	−1.2 ± 33.8	0.1 ± 0.0

allows for efficient processing of the shmiR into functional effector siRNAs with reduced heterogeneity. The increased efficiency is due to a more stringent nuclear cleavage by Drosha.[25] Furthermore, in the BB-301 vector, the skeletal and cardiac muscle-specific promoter Spc5-12, which is an RNA II polymerase promoter, drives the expression of the shmiRs as well as the codon-optimized PABPN1 gene, which further enhances safety of the vector.

One potential concern surrounding a single "silence and replace"-based vector is the relative expression levels of the individual components. The processed siRNAs in this system are unable to discriminate between the wild-type and mutant allele, which results in downregulation of all endogenous PABPN1 mRNA and protein. At the same time, sufficient expression of the codon-optimized PABPN1 is required, particularly since this protein plays a critical role in mRNA regulation. PABPN1 expression is very low in skeletal muscle.[5] Therefore, there is no need for high-level expression of PABPN1 to have a physiological effect in treated muscle. Accordingly, in our study, as outlined in Table 1, BB-301 mid-range doses of 1×10^{10} and 5×10^{10} vg/muscle demonstrated an ~32% inhibition of wild-type and mutant PABPN1 in A17 mice, with a quite modest replacement index of 1%–2%. Yet, these mid-range doses were able to significantly reduce the accumulation of INIs as well as partially restore both muscle strength and muscle weight. Additionally, there were no overt negative clinical findings observed in any of the animals at any administered dose related to administration of the gene therapy. At the second highest dose of BB-301, 2.5×10^{11} vg/muscle, we observed a full restoration to wild-type levels of all phenotypic parameters related to INIs, muscle strength, and weight with silence and replace indices of 75% and 26%, respectively. We therefore conclude that both a low level of protein expression and duration of treatment can support enhanced enzymatic and physiological function. Furthermore, the ability of partial mutant PABPN1 expression inhibition and partial restoration of PABPN1 function via expression of coPABPN1 suggests that even low levels of transduction *in vivo* may provide a physiological and histological benefit and may bode well for a broad response range in a human clinical setting.

In this proof-of-concept pre-clinical study in mice, we used intramuscular injection in TA muscle, since TA muscle allows an easy access and downstream functional physiological evaluations. Additionally, we have previously demonstrated that the TA muscle of the A17 mouse is relevant to study effect on OPMD muscles: TA muscle features include muscle weakness, fiber atrophy, fibrosis, and PABPN1 aggregates as seen in human OPMD muscles.[26] Future pre-clinical studies in larger animals should be done in muscles of the pharyngeal area to demonstrate successful administration of the drug to the affected area in patients. This study demonstrates that local administration of BB-301 has a beneficial impact on pathology and muscle function in the A17 mouse model. In humans the muscles of both the eyelids and pharyngeal area have the most severe pathology in OPMD, while other muscles (in particular, those of the proximal limbs) are progressively affected. Ptosis (eyelid drooping) can be surgically corrected. Dysphagia (difficulty in swallowing) impacts patients the most. As the disease progresses, symptoms associated with dysphagia worsen and palliative treatments like cricopharyngeal dilation or myotomy are performed.[3] Not surprisingly, the effects of these treatments are temporary in nature, since the genetic defect is still present in the muscles. The vector BB-301 could be administered locally to the muscles of the tongue or pharyngeal muscles that coordinate and control swallowing to correct muscle pathology and function in this area, with the potential for lasting benefit in patients with OPMD. At present, pre-clinical studies are ongoing in a dog model that aim to develop and evaluate administration to muscles of the pharyngeal complex. Systemic administration of the BB-301 to OPMD patients can be considered as well. Such administration poses technical challenges, however, in that the human liver acts as a sink for systemic administered viral vectors and would somehow need to be avoided. Also, systemic administration to transduce all muscle groups of the human body would also require high doses of AAV vector, likely in excess of 10^{15} viral genomes total per administration, which may trigger toxicity as has been observed in animal models.[27]

All these features suggest that the BB-301 vector is safe and effective. It has received the orphan drug designation from EMEA and FDA and is currently being prepared for administration in human patients.

MATERIALS AND METHODS
Cell lines
Human embryonic kidney cells (HEK293, ATCC, catalog no. CRL-1573) were grown in Dulbecco's modified Eagle's medium (DMEM, Gibco, catalog no. 11995065) containing 20 mM HEPES,
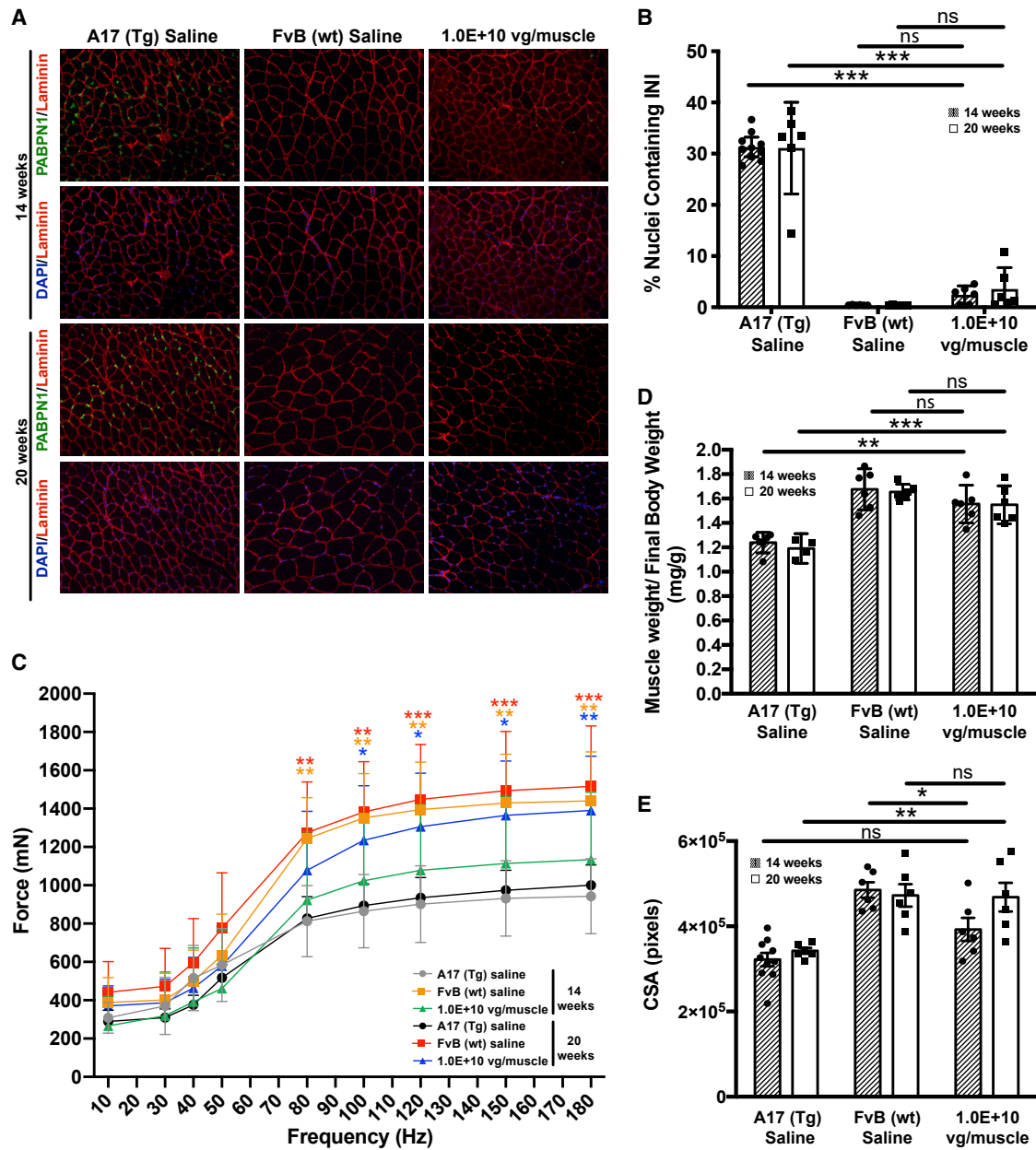
Figure 5. Longer treatment with BB-301 is more effective in A17 mice

(A) Immunofluorescence of PABPN1 (green) and laminin (red) in sections of treated muscles. Sections were pre-treated with 1 M KCl to remove all soluble aggregates from the tissue. (B) Quantification of percentage of nuclei containing INIs in muscle sections indicates that treatment with 1×10^{10} vg/TA muscle of BB-301 efficiently reduces INIs by 80% compared with saline-injected A17 mice. (C) Maximal force generated by TA muscles of BB-301 treated mice at 14 and 20 weeks was measured by *in situ* muscle physiology and compared to saline-treated A17 mice. At 14 weeks the treatment already increased the maximal force generated by TA muscles. The maximal force was further increased from 14 to 20 weeks in BB-301-treated TA muscles. (D) The ratio of muscle weight to body weight shows that the muscle mass is recovered after 14 weeks of treatment. (E) Analysis of the cross-sectional area of treated TA muscles shows that treatment with 1×10^{10} vg/TA muscle of BB-301 for 20 weeks normalizes the width of muscle fibers to wild-type levels. Data are presented as mean ± 95% confidence interval. Sample size ranged from four to six TA muscles per dosing group as indicated by the dot plot. Mixed-effects analysis with Tukey multiple comparison test was used for data analysis. *p < 0.05, **p < 0.01, ***p < 0.001; ns, not significant.

10% fetal bovine serum (FBS, Gibco, catalog no. 16000044), and 2 mM L-glutamine (Gibco, catalog no. 25030081) in a humidified, 5% CO_2 air atmosphere at 37°C.

shmiR design

Prior to shmiR sequence design and selection, a Clustal W2 alignment was performed on the corresponding reference complementary DNA

(cDNA) of PABPN1 from human, mouse, bovine, ovine, dog, and a non-human primate species to define targetable sequences with a high degree of identity between all species. In addition, the siRNAs were aligned against sequences that encode the codon-optimized PABPN1 to ensure that the siRNA target regions did not have high levels of identity in the codon-optimized PABPN1. A list containing dozens of potential candidate sequences was identified and ultimately narrowed down to 17 that were selected for further empirical testing. The sequences encoding each siRNA are maintained as a perfectly matched duplex with the exception of the 5' end, in which the first nucleotide of the top strand is modeled into a bulge structure immediately preceding the duplex (sequences listed in Table S2). The siRNA sequence is flanked by miR-30A stem structure on one side and a loop sequence on the other. Finally, the virtual constructs were run through an mFold analysis (https://www.rna.albany.edu/unafold-web-server-discontinued) to ensure that the hairpin structures maintain the expected conformation. Once cloned under the control of the U6-1, a strong and constitutively active Pol III promoter used for screening the candidates, the resulting constructs have been termed shmiR sequences.

qRT-PCR analysis

Total RNA was extracted from skeletal muscles with the RNeasy Fibrous Tissue Mini Kit (QIAGEN, catalog no. 74704) according to the manufacturer's instructions. Quality and purity of the RNA were accessed with a NanoDrop 1000 spectrophotometer (Thermo Fisher Scientific, Waltham, MA, USA). First-strand cDNA synthesis was reverse transcribed from 100 ng of purified RNA using random hexamer primers with the High-Capacity cDNA Reverse Transcription Kit (Thermo Fisher Scientific, catalog no. 4374966) per manufacturer's instructions. qPCR analysis was performed with TaqMan primers and probes targeting wtPABPN1 (forward: 5′-ATGGTGCAAC AGCAGAAGAG-3', reverse: 5′-CTTTGGGGATGGCCACTAAAT-3', and probe: 5′-FAM-CGGTTGACTGAACCACAGCCATG-BHQ-3'), coPABPN1 (forward: 5′-ACCGACAGAGGCTTCCCCTA-3′, reverse: 5′-TTCTGCTGCTGTTGTAGTTGG-3′, and probe: 5′-FAM-TGG TCCGGGCTCTGTACCTAGCC-BHQ-3′) or GAPDH TaqMan gene expression assay (Thermo Fisher Scientific, catalog no. Hs02758991_g1). The mixture of qPCR reaction was 2 μL of cDNA, 1× TaqMan assay or 1 μM forward primer, 1 μM reverse primer, 200 nM probe, and 1× Maxima Probe/ROX qPCR Master Mix (Thermo Fisher Scientific, catalog no. K0231) in a 10 μL total reaction volume. The reactions were carried out on an ABI 7900 or QuantStudio 5 real-time PCR machine with settings of 50°C for 2 min, 95°C for 10 min, 95°C for 15 s/60°C for 1 min: 40 cycles. The expression level of PABPN1 was normalized to that of murine GAPDH mRNA expression.

siRNA copy number analysis

For siRNA copy number analysis, custom RT and qPCR assays were developed for each shmiR used in the study. First, a standard curve was generated for each hairpin utilizing a 10-fold dilution series (10^8–10^2 copies) of high-pressure liquid chromatography (HPLC)-purified RNA oligos (Sigma-Aldrich). Sequence for

siRNA13 oligo is 5′-AGGGGAAUACCAUGAUGUCGC-3′ and for siRNA17 oligo is 5′- UUCAUCUGCUUCUCUACCUC-3′. Next, diluted RNA oligo standards and 50 ng of purified RNA from each TA muscle sample were reverse transcribed into cDNA with the miScript II RT Kit (QIAGEN, catalog 218161). RT reaction mix consisted of 50 ng of RNA, 1× miScript HiSpec Buffer, 1× miScript nucleic acid mix, and 1× miScript reverse transcriptase mix in a 10 μL reaction volume. RT reaction was carried out on a regular PCR machine with settings of 37°C for 60 min, 95°C for 5 min. Finally, qPCR assay was performed with the miScript SYBR Green PCR Kit (QIAGEN, catalog no. 218073) with reaction mixture of 2 μL of 1:10 dilution of cDNA, 1× Quantitect SYBR mix, 1× of miScript universal primer, and 4 μM forward primer in a 10 μL reaction volume. Forward primer sequence for siRNA13 is 5′-AGGGGAATACCATGATGTCGC-3′ and for siRNA17 is 5′-ATTCATCTGCTTCTCTACCTC-3′. The reactions were carried out on ABI 7900 or QuantStudio 5 real-time PCR machine with settings of 95°C for 10 min, 94°C for 15 s, 55°C for 30 s, 70°C for 30 s for 45 cycles. The absolute amount of siRNA copies was calculated using standard curves prepared for each individual siRNA.

Western blot

A total of 20 μg of protein was mixed with reducing agent and sample loading buffer in a total volume of 40 μL and then loaded onto a 4%–12% NuPage Bis-Tris gel (Invitrogen, catalog no. NP0327BOX). Five microliters of SeeBlue Plus2 pre-stained protein standard (Life Technologies, catalog no. LC5925) was also loaded onto the gel. The gel was run in 1× MES Running Buffer (Life Technologies, catalog no. B0002) for 30–45 min at 200 V. Upon completion of gel electrophoresis, the protein gel was transferred to a iBlot polyvinylidene fluoride (PVDF) membrane (Life Technologies, catalog IB24001) at 20 V for 1 h. With the iBind Western System (Life Technologies, catalog no. SLF1000S), anti-ddk primary antibody (OriGene, catalog no. TA50011-100) and anti-mouse secondary antibody (Sigma, catalog no. A3562) were added to the device at dilutions of 1:500 and 1:6,000, respectively. Anti-HSP90 antibody (catalog no. SAB4200812) was purchased from Sigma. The membrane was incubated overnight and then rinsed with water and visualized with 9H-(1,3-dichloro-9,9-dimethylacridin-2-one-7-yl) (DDAO) Phosphate Buffer (10 mM Tris pH 9.5, 1 mM $MgCl_2$) and DDAO dye (Invitrogen, catalog no. D6487). Briefly, 20 mL of $DDAOPO_4$ base buffer and 20 μL of DDAO dye were mixed together (a 1:1, 000 dilution). Five milliliters of the DDAO mixture was pipetted onto a plastic sheet, and the membrane was placed on top of the dye mixture with protein side down at room temperature for 1–15 min (depending on the expected level of expression). The membrane was read on a Fujifilm FLA-3000 Phosphoimager at 633 nm.

NGS analyses and siRNA transfection

For NGS analysis, 300–500 ng of RNA purified from BB-301-infected TA muscles with the RNeasy Fibrous Tissue Mini Kit (QIAGEN, catalog no. 74704) was sent to SeqMatic (Fremont, CA, USA). Libraries were prepared with the SeqMatic TailorMix miRNA Sample

Preparation Kit V2 (SeqMatic SKU: TM302-A) and analyzed with Illumina NextSeq500 at the High output (1 × 75 bp) setting. Approximately 40 million reads were generated per library. Sequencing adapters and reads of low quality were trimmed using Cutadapt. The program was set with a minimum read length of 16 nt and a quality score cutoff of PHRED score Q20.[28] Clean reads were mapped to full-length siRNA sequences with Bowtie1. The percentages of reads based on the total number of reads matching the reference sequence were calculated (Figure S1A).

Synthetic siRNAs for all species identified in the NGS analysis were purchased from Dharmacon (Chicago, IL, USA). Sequences for each siRNA tested are listed in Table S3. Five picomoles of siRNA was transfected into HEK293 cells (1e5 cells) in a 24-well plate with Lipofectamine RNAiMax reagent according to the manufacturer's protocol (Thermo Fisher Scientific, catalog no. 13778100). ON-TARGETplus non-targeting siRNA #1 was used as negative control (Dharmacon, catalog no. D-001810-01-05). After a 48-h incubation, RNA was extracted with the miRNeasy Mini Kit (QIAGEN, catalog no. 217004). wtPABPN1 inhibition was analyzed by qRT-PCR analysis using the abovementioned conditions. Percent inhibition was calculated as relative wtPABPN1 expression to the siRNA negative control.

Manufacture of AAV

AAV was generated with the baculovirus insect cell production system. Amino acid substitutions within the phospholipase domain[17] were generated to restore the phospholipase activity in the AAV9 capsid. Mutations introduced into the AAV9 VP1 sequence were 56 G to F, 67 A to E, 81 Q to R, 84 K to D, and 85 A to S. These modifications were essential to obtaining high-yield, functional AAV with the baculovirus insect system. The phospholipase activity enables the virus to escape from endosomes and next deliver the payload to the nucleus.

To generate BB-301 AAV, growing Sf9 insect cells in Sf-900II SFM medium (Thermo Fisher, catalog no. 10902-088) were coinfected with 0.1 MOI of each Baculo-AAV9PL (containing sequence for rep/cap) and Baculo-BB-301 (containing the sequence for the gene of interest and both siRNA 13 and 17). After a 6-day production period in shaker flasks at 28°C, cells and cell debris were removed through centrifugation (15 min at 2,000 × g) before the AAV-containing supernatant was clarified through a series of 0.2- and 0.1-micron filters (Nalgene bottle top filters, catalog nos. 569-0020 and 567-0010, respectively). The AAV virus was concentrated by precipitation at 2°C–8°C overnight with a final concentration of 8% (w/v) PEG 8000 (VWR, catalog no. 0159)/0.5 M NaCl solution. The precipitation was pelleted through centrifugation (45 min at 4°C, 2,500 × g). The virus-containing pellet was resuspended in buffer (50 mM Tris-HCl, 150 mM NaCl, and 2 mM MgCl$_2$, pH 8.0) and purified further on an iodixanol gradient of layered 60%, 40%, 25%, and 15% iodixanol (OptiPrep, Cosmo Bio, catalog no. AXS-1114542) and centrifuged at 18°C at 350,000 × g for 1 h. The AAV-enriched, 40% iodixanol layer was polished further by a cesium chloride gradient ultracentrifugation step using a final 1.38 g/mL cesium chloride density in the final sample/cesium chloride tube and

centrifuged at 4°C and 350,000 × g for 24 h. The separated bands were recovered individually, and the band with the enriched full capsid BB-301 product was buffer exchanged seven times into proprietary formulation buffer using Amicon centrifugal filter units at 4,000 × g (Millipore, catalog no. UFC910024). The formulated BB-301 was 0.22-micron sterile filtered (Pall syringe filter, catalog no. 4187) before aliquots were stored frozen for usage in animal experiments and quality analysis, including AAV concentration. The AAV vector genome concentration, expressed in vg/mL, was determined with a real-time quantitative TaqMan PCR (qPCR). Here, the primer/probe pairs targeting a segment in the transgene of the viral genome were amplified and quantified using a plasmid standard carrying the same DNA segment of known concentrations (copies/mL).

In vivo experiments

A17.1 transgenic mice (here called A17) were provided by Dr. David Rubinsztein's laboratory and have previously been described.[13,26] They are also commercially available from the Jackson Laboratory: FvB-Tg (ACTA1-PABPN1*A17) 1Drub/DrubJ, Stock No: 016193. A17 mice and wild-type FvB controls were generated by crossing the heterozygous carrier strain A17 with the FvB background mice and genotyped by PCR for bovine PABPN1 4 weeks after birth. The following primers were used to amplify the expanded bovine PABPN1 and the housekeeping gene 18S: for bovine PABPN1: forward 5′-GAACCAACAGACCAGGCATC-3' and reverse 5′- GTGATGGTGATGATGACCGG-3a′; for 18S: forward 5′-TTGACGGAAGGGCACCACCAG-3′, and reverse 5′-GCACCACCACCCACGGAATCG-3′. One microliter of extracted DNA was used for the PCR (40 cycles: 95°C for 30 s, 60°C for 30 s, and 72°C for 30 s). Animals were housed with food and water *ad libitum* in minimal disease facilities (Royal Holloway, University of London).

In vivo experiments were conducted under statutory Home Office recommendation; regulatory, ethics, and licensing procedures; and the Animals (Scientific Procedures) Act 1986. Briefly, 10- to 12-week-old A17 mice were anesthetized with isoflurane. In the dose range finding studies, six different doses of BB-301 ranging from 4 × 10^8 vg/muscle to 7.5 × 10^{11} vg/muscle were diluted in saline and were administered intramuscularly as 50 μL volumes in each TA muscle of the mice. Saline-injected TA of both A17 mice and FvB mice were used as negative and healthy controls, respectively. For each dosing group, five male mice and two TA muscles from each mouse were dosed. At 14 weeks post-injection, mice were anesthetized with intraperitoneal injection of a mix of Hypnorm (VetaPharma, Elmet, UK, catalog no. Vm41760/4000) and Hypnovel (Roche, catalog no. 59467-70-8) solution, and *in situ* TA muscle physiology was performed. After analysis, mice were sacrificed and TA muscles were excised, weighed, and frozen in liquid nitrogen-cooled isopentane. For the time course study, mice were injected with a dose of BB-301 at 1 × 10^{10} vg/muscle or 6 × 10^{10} vg/muscle. For each dosing group, three male mice and two TA muscles from each mouse were dosed. Different cohorts of mice were sacrificed at either 14 weeks or 20 weeks time points.

Muscle force measurement

Contractile properties of TA muscles were analyzed by *in situ* muscle electrophysiology.[21] A blind analysis was performed by the investigator. The knee and foot were fixed with clamps, and the distal tendons of the muscles were attached to a dual-mode servomotor transducer (Aurora Scientific, Aurora, ON, Canada, catalog no. 305B) with a 4.0 braided surgical silk (Interfocus, Cambridge, UK, catalog no. 18020-40). The sciatic nerves were proximally crushed and distally stimulated by a bipolar silver electrode using supramaximal square-wave pulses of 0.02 ms duration (stimulator, Aurora Scientific, catalog no. 701A). All data provided by the isometric transducer were recorded and analyzed with a LabVIEW-based DMC program (Dynamic Muscle Control and Data Acquisition; Aurora Scientific). All isometric measurements were made at an initial length L0 (length at which maximal tension was obtained during the tetanus). Response to tetanic stimulation (9 pulse frequencies ranging from 10 to 150 Hz) was recorded, and the maximal force was determined. The length of the muscle was measured with a caliper. After contractile measurements, the muscles were collected and weighed to calculate the specific maximal force, frozen in isopentane cooled in liquid nitrogen, and stored at $-80°C$.

Immunofluorescence

Muscle tissue sections of were cut at 10 μm thickness with a Bright OTF 5000 cryostat (Bright Instruments, Huntingdon, UK). They were placed on coated glass slides (VWR, Lutterworth, UK) and stored at $-80°C$ prior to use. For immunohistochemical staining the following antibodies were used: anti-PABPN1 (rabbit monoclonal, diluted 1:100, Abcam ab75855, overnight at 4°C) and anti-Laminin (rat monoclonal; diluted 1:800; Sigma-Aldrich, catalog no. L0663 Gillingham, UK, 1 h at room temperature). Secondary antibodies were Alexa Fluor conjugated to 488 (Life Technologies catalog no. A-11034) or 594 (Life Technologies catalog no. A-11005) fluorochromes. PABPN1-positive intranuclear inclusions were detected with a previously published protocol.[12] Briefly, muscle sections were fixed in paraformaldehyde 4% for 10 min, and soluble proteins were removed by incubating slides with KCl buffer (1 M KCl, 30 mM HEPES, 65 mM PIPES, 10 mM EDTA, 2 mM $MgCl_2$, pH 6.9) for 1 h at room temperature. Tissue sections were then blocked with 1% normal goat serum in 0.1 M phosphate-buffered saline (PBS), 0.1% Triton X-100 for 1 h and then incubated overnight at 4°C with anti-PABPN1 and anti-Laminin primary antibodies diluted in the same buffer. After washings, sections were incubated with fluorophore-conjugated secondary antibodies. Finally, slides were incubated with 4′,6-diamidino-2-phenylindole (DAPI, 3 μg/mL; Sigma-Aldrich, Gillingham, UK, catalog no. D9542) for 5 min and mounted with Mowiol. To analyze the INI content, the largest section per each muscle was considered; five fields (at 20× magnification) were randomly captured per each muscle (covering more than ∼80% of the total muscle section area). Fields had on average ∼250 nuclei in saline-treated FvB (larger fibers, fewer nuclei per field) and ∼350 nuclei in saline-treated A17 (atrophic fibers, more nuclei per field). This means that on average between 1,000 and 2,000 nuclei were counted per TA sample. All immunofluorescence images were captured and digitized using identical parameters of exposure, saturation, and gamma-levels between specimens. INI and nuclei were manually counted with NIH ImageJ analysis software (NIH, Bethesda, MD, USA), and the ratio INI/nuclei was calculated. On average 1,000–2,000 nuclei per TA sample were counted and evaluated.

Statistical analysis

All data are presented as mean values ± 95% confidence interval. Number of samples for each dosing group is presented as dot plot in figures. Dependent on whether a single or multiple time points were analyzed, either two-way ANOVA or mixed-effects analysis to account for repeated measures was applied. Statistical analyses with the Tukey multiple comparison test were performed with GraphPad Prism version 8.0 (GraphPad Software, San Diego, CA, USA). A difference was considered to be significant at $*p < 0.05$, $**p < 0.01$, $***p < 0.001$.

SUPPLEMENTAL INFORMATION

Supplemental information can be found online at https://doi.org/10.1016/j.omtn.2021.02.017.

AUTHOR CONTRIBUTIONS

D.S., V.S.-U., S.H., P.R., A.M., C.T., and G.D. devised the BB-301 molecular construct. P.R. devised the modified AAV9 vector. V.S. and S.H. constructed BB-301 and performed *in vitro* testing that included analyses of protein levels and mRNA levels as well as the testing regarding shmiR processing and siRNA confirmation. V.S.-U. designed the qPCR assays used to detect the siRNA produced by each shmiR. V.S., S.H., S.-C.K., K.T., and C.K. were responsible for AAV production and method development for baculovirus-based AAV production. D.S., V.S.-U., A.M., C.T., and G.D. conceived and designed the animal studies. A.M., F.R., O.C., N.L.-N., C.T., and G.D. performed all of the in-life animal work as well as post-life analyses for intranuclear inclusions, muscle strength, and muscle weight. V.S.-U. and S.H. performed all the quantitative aspects of siRNA expression and codon-optimized protein expression in the post-life tissues. D.S., C.T., G.D., V.S.-U., A.M., S.H., G.K., P.R., S.-C.K., and S.M. were responsible for data analyses and for writing the manuscript.

DECLARATION OF INTERESTS

V.S., S.H., K.T., and D.S. are former employees of Benitec Biopharma. S.-C.K., C.K., S.M., and P.R. are current employees of Benitec Biopharma and have financial interest in the development of BB-301

products. A patent named "Reagents for treatment of oculopharyngeal muscular dystrophy (OPMD) and use thereof" has been filed by Benitec Biopharma and includes D.S., A.M., G.D., and C.T. as named inventors. All other authors have no conflict of interest.

REFERENCES

1. Duranceau, C.A., Letendre, J., Clermont, R.J., Lévesque, H.P., and Barbeau, A. (1978). Oropharyngeal dysphagia in patients with oculopharyngeal muscular dystrophy. Can. J. Surg. *21*, 326–329.

2. Périé, S., Eymard, B., Laccourreye, L., Chaussade, S., Fardeau, M., and Lacau St Guily, J. (1997). Dysphagia in oculopharyngeal muscular dystrophy: a series of 22 French cases. Neuromuscul. Disord. *7* (Suppl 1), S96–S99.

3. Trollet, C., Gidaro, T., Klein, P., Perie, S., Butler-Browne, G., and Lacau St Guily, J. (2014). Oculopharyngeal Muscular Dystrophy. In Gene Reviews, M.P. Adam, H.H. Ardinger, R.A. Pagon, S.E. Wallace, L.J.H. Bean, K. Stephens, and A. Amemiya, eds. (University of Washington), pp. 1–20.

4. Brais, B., Bouchard, J.P., Xie, Y.G., Rochefort, D.L., Chrétien, N., Tomé, F.M., Lafrenière, R.G., Rommens, J.M., Uyama, E., Nohira, O., et al. (1998). Short GCG expansions in the PABP2 gene cause oculopharyngeal muscular dystrophy. Nat. Genet. *18*, 164–167.

5. Apponi, L.H., Corbett, A.H., and Pavlath, G.K. (2013). Control of mRNA stability contributes to low levels of nuclear poly(A) binding protein 1 (PABPN1) in skeletal muscle. Skelet. Muscle *3*, 23.

6. Jouan, L., Rocheford, D., Szuto, A., Carney, E., David, K., Dion, P.A., and Rouleau, G.A. (2014). An 18 alanine repeat in a severe form of oculopharyngeal muscular dystrophy. Can. J. Neurol. Sci. *41*, 508–511.

7. Tomé, F.M., and Fardeau, M. (1980). Nuclear inclusions in oculopharyngeal dystrophy. Acta Neuropathol. *49*, 85–87.

8. Gidaro, T., Negroni, E., Périé, S., Mirabella, M., Lainé, J., Lacau St Guily, J., Butler-Browne, G., Mouly, V., and Trollet, C. (2013). Atrophy, fibrosis, and increased PAX7-positive cells in pharyngeal muscles of oculopharyngeal muscular dystrophy patients. J. Neuropathol. Exp. Neurol. *72*, 234–243.

9. Banerjee, A., Vest, K.E., Pavlath, G.K., and Corbett, A.H. (2017). Nuclear poly(A) binding protein 1 (PABPN1) and Matrin3 interact in muscle cells and regulate RNA processing. Nucleic Acids Res. *45*, 10706–10725.

10. Anvar, S.Y., Raz, Y., Verway, N., van der Sluijs, B., Venema, A., Goeman, J.J., Vissing, J., van der Maarel, S.M., 't Hoen, P.A.C., van Engelen, B.G.M., and Raz, V. (2013). A decline in PABPN1 induces progressive muscle weakness in oculopharyngeal muscle dystrophy and in muscle aging. Aging (Albany NY) *5*, 412–426.

11. Vest, K.E., Phillips, B.L., Banerjee, A., Apponi, L.H., Dammer, E.B., Xu, W., Zheng, D., Yu, J., Tian, B., Pavlath, G.K., and Corbett, A.H. (2017). Novel mouse models of oculopharyngeal muscular dystrophy (OPMD) reveal early onset mitochondrial defects and suggest loss of PABPN1 may contribute to pathology. Hum. Mol. Genet. *26*, 3235–3252.

12. Malerba, A., Klein, P., Bachtarzi, H., Jarmin, S.A., Cordova, G., Ferry, A., Strings, V., Espinoza, M.P., Mamchaoui, K., Blumen, S.C., et al. (2017). PABPN1 gene therapy for oculopharyngeal muscular dystrophy. Nat. Commun. *8*, 14848.

13. Davies, J.E., Wang, L., Garcia-Oroz, L., Cook, L.J., Vacher, C., O'Donovan, D.G., and Rubinsztein, D.C. (2005). Doxycycline attenuates and delays toxicity of the oculopharyngeal muscular dystrophy mutation in transgenic mice. Nat. Med. *11*, 672–677.

14. Chartier, A., Klein, P., Pierson, S., Barbezier, N., Gidaro, T., Casas, F., Carberry, S., Dowling, P., Maynadier, L., Bellec, M., et al. (2015). Mitochondrial dysfunction reveals the role of mRNA poly(A) tail regulation in oculopharyngeal muscular dystrophy pathogenesis. PLoS Genet. *11*, e1005092.

15. Li, X., Eastman, E.M., Schwartz, R.J., and Draghia-Akli, R. (1999). Synthetic muscle promoters: activities exceeding naturally occurring regulatory sequences. Nat. Biotechnol. *17*, 241–245.

16. Draghia-Akli, R., Fiorotto, M.L., Hill, L.A., Malone, P.B., Deaver, D.R., and Schwartz, R.J. (1999). Myogenic expression of an injectable protease-resistant growth hormone-releasing hormone augments long-term growth in pigs. Nat. Biotechnol. *17*, 1179–1183.

17. Popa-Wagner, R., Porwal, M., Kann, M., Reuss, M., Weimer, M., Florin, L., and Kleinschmidt, J.A. (2012). Impact of VP1-specific protein sequence motifs on adeno-associated virus type 2 intracellular trafficking and nuclear entry. J. Virol. *86*, 9163–9174.

18. Kohlbrenner, E., Aslanidi, G., Nash, K., Shklyaev, S., Campbell-Thompson, M., Byrne, B.J., Snyder, R.O., Muzyczka, N., Warrington, K.H., Jr., and Zolotukhin, S. (2005). Successful production of pseudotyped rAAV vectors using a modified baculovirus expression system. Mol. Ther. *12*, 1217–1225.

19. Denise, H., Moschos, S.A., Sidders, B., Burden, F., Perkins, H., Carter, N., Stroud, T., Kennedy, M., Fancy, S.-A., Lapthorn, C., et al. (2014). Deep sequencing insights in therapeutic shRNA processing and siRNA target cleavage precision. Mol. Ther. Nucleic Acids *3*, e145.

20. Suhy, D.A., Kao, S.C., Mao, T., Whiteley, L., Denise, H., Souberbielle, B., Burdick, A.D., Hayes, K., Wright, J.F., Lavender, H., et al. (2012). Safe, long-term hepatic expression of anti-HCV shRNA in a nonhuman primate model. Mol. Ther. *20*, 1737–1749.

21. Vignaud, A., Ramond, F., Hourdé, C., Keller, A., Butler-Browne, G., and Ferry, A. (2007). Diabetes provides an unfavorable environment for muscle mass and function after muscle injury in mice. Pathobiology *74*, 291–300.

22. Li, C., Xiao, P., Gray, S.J., Weinberg, M.S., and Samulski, R.J. (2011). Combination therapy utilizing shRNA knockdown and an optimized resistant transgene for rescue of diseases caused by misfolded proteins. Proc. Natl. Acad. Sci. USA *108*, 14258–14263.

23. Borel, F., Tang, Q., Gernoux, G., Greer, C., Wang, Z., Barzel, A., Kay, M.A., Shultz, L.D., Greiner, D.L., Flotte, T.R., et al. (2017). Survival Advantage of Both Human Hepatocyte Xenografts and Genome-Edited Hepatocytes for Treatment of α-1 Antitrypsin Deficiency. Mol. Ther. *25*, 2477–2489.

24. Cideciyan, A.V., Sudharsan, R., Dufour, V.L., Massengill, M.T., Iwabe, S., Swider, M., Lisi, B., Sumaroka, A., Marinho, L.F., Appelbaum, T., et al. (2018). Mutation-independent rhodopsin gene therapy by knockdown and replacement with a single AAV vector. Proc. Natl. Acad. Sci. USA *115*, E8547–E8556.

25. McBride, J.L., Boudreau, R.L., Harper, S.Q., Staber, P.D., Monteys, A.M., Martins, I., Gilmore, B.L., Burstein, H., Peluso, R.W., Polisky, B., et al. (2008). Artificial miRNAs mitigate shRNA-mediated toxicity in the brain: implications for the therapeutic development of RNAi. Proc. Natl. Acad. Sci. USA *105*, 5868–5873.

26. Trollet, C., Anvar, S.Y., Venema, A., Hargreaves, I.P., Foster, K., Vignaud, A., Ferry, A., Negroni, E., Hourde, C., Baraibar, M.A., et al. (2010). Molecular and phenotypic characterization of a mouse model of oculopharyngeal muscular dystrophy reveals severe muscular atrophy restricted to fast glycolytic fibres. Hum. Mol. Genet. *19*, 2191–2207.

27. Hinderer, C., Katz, N., Buza, E.L., Dyer, C., Goode, T., Bell, P., Richman, L.K., and Wilson, J.M. (2018). Severe Toxicity in Nonhuman Primates and Piglets Following High-Dose Intravenous Administration of an Adeno-Associated Virus Vector Expressing Human SMN. Hum. Gene Ther. *29*, 285–298.

28. Martin, M. (2011). Cutadapt Removes Adapter Sequences From High-Throughput Sequencing Reads. EMBnet. J. *17*, 10–12.